euronoise

Tactile Touch Plate with Variable Boundary Conditions

Ros Kiri Ing[a], Didier Cassereau[b], Mathias Fink[a] and Jean-Pierre Nikolovski[a]

[a]Laboratoire Ondes et Acoustique, ESPCI, Université Paris 7, CNRS, 10 rue Vauquelin, 75005 Paris, France
[b]Laboratoire Ondes et Acoustique, 10, rue Vauquelin, 75231 Paris, France
ros-kiri.ing@espci.fr

The touch screen device is becoming more and more widespread because it is a very user friendly human/machine interface. In acoustic domains, several approaches are used to realize such a device. Triangulation or Rayleigh waves absorption are such classical methods. However, these approaches are limited because they need a large number of sensors and are only applicable to plates of constant thickness and homogeneous materials. To remedy these limitations, a new approach is proposed using only two sensors. In this approach, one sensor is used to excite the plate, either continuously or impulsively. The second sensor is used to detect the acoustic waves generated in the plate. When a human finger comes into contact with the plate, some acoustic wave characteristics change. These changes affect different frequencies and depend on the position of the contact point. Comparing these changes with pre-recorded values, it is possible to achieve a tactile touch device that only responds to specific touch locations.

1 Introduction

Since the first patent in 1972 [1] concerning a tactile interface based on acoustic waves, the technology has been significantly improved. Unfortunately, the systems that have been developed until now are complex [2] or require a large number of transducers [3]. Recently, a passive approach [4,5] based on the cross-correlation of acoustic signals has been proposed, that needs only one transducer, and does not require any change of the tactile object itself. The inconvenient of this approach is that it is expensive in terms of computation time, due to the evaluation of cross-correlations of signals made of 512 or 1024 samples. In this paper, we present a simplified alternate method based on the selective absorption of the vibration modes of the object. With this new technique, the number of physical parameters to compare is significantly reduced, up to a ratio of 10. In order to simplify, the approach is presented here in the case of a 1D bar, but it can be extended to plates of variable geometry, thickness and/or shape.

2 Vibration of a bar

The vibration of a bar follows three different modes: bending, compression and torsion. The generation of one or several of these modes depends on the position of the source and on the excitation source type. A point-like source, located at the half thickness and half width on one side of the bar, that applies a strength parallel to the bar, generates the compression mode only. A point-like source located in the middle of the bar and normal to its surface mainly generates the bending mode. Last, a source located outside the symmetry axis of the bar is able to generate the torsion mode. The amplitudes of the vibration modes generated in the bar depend on the location of the source, but also on its surface properties as well as on its frequency spectrum. These amplitudes also depend on the boundary conditions that are applied at each end of the bar, that can be free of fixed.

In this work, we are interested in the bending mode because it is highly sensitive to the conditions on the surface of the bar. In our experiment, the bar is made of Duralumin (Fig. 1). The vibrations are measured with a laser vibrometer. The source excitation is generated with a small hammer to generate a point-like source (at 1 mm from the right end of the bar) or with a small piezoelectric sensor – usually found in consumer electronic products - of 8 mm diameter centered at 11 mm from the right end of the bar. The bar is supported by two foam cubes of weak density, such that it can vibrate as a free body.

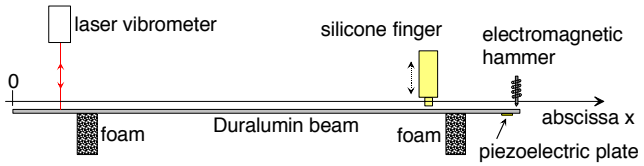

Figure 1: Experimental setup.

The modeling of the bar is based on the Bernouilli assumption, that considers that its thickness is small enough to be neglected compared to the two other dimensions. The amplitude of the vibration of the bending mode, measured along the normal direction to the bar, satisfies the following equation [6]:

$$\rho S \frac{\partial^2 w}{\partial t^2} + EI \frac{\partial^4 w}{\partial x^4} = F_2 - \frac{\partial M_3}{\partial x} \qquad (1)$$

where

E: Young modulus,

I: quadratic moment,

ρ: volume density,

S: section,

F_2: normal excitation force,

M_3: bending moment of the excitation.

The vibration modes of the bar are obtained from particular solutions written as $w(x,t)=W(x)\ e^{j\omega t}$; this yields a new equation for $W(x)$, whose solution without excitation term is:

$$W(x) = A\sin(\beta s) + B\cos(\beta s) + C\sinh(\beta s) + D\cosh(\beta s) \qquad (2)$$

where $\beta^4=\rho S\omega(EI)^{-1}$.

We suppose here that the two ends of the bar are free. From the boundary conditions satisfied by the bending moments and stresses at each end, we obtain a linear and homogeneous system of 4 equations for the 4 unknown parameters A, B, C and D (the right-hand side of this system is 0). The determinant of this system must be zero in order to ensure the existence of vibration modes in the bar ; this

condition allows to calculate the eigen wavelengths of the bar β_m ; for each value of β_m, the eigenvectors leads to the determination of the corresponding coefficients A_m, B_m, C_m and D_m that characterize the amplitude of the vibration for the mode m of the bar.

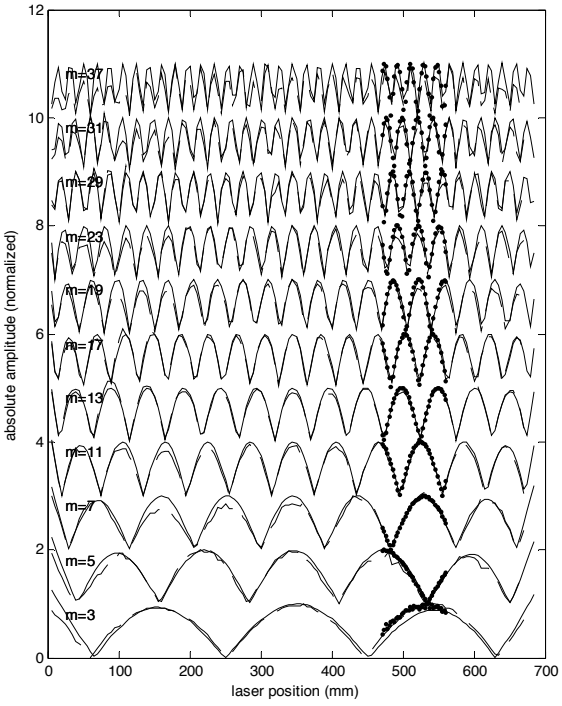

Figure 2: Normalized absolute amplitudes of arbitrary chosen modes ; theory (continuous lines) and experiment (dotted and dashed lines).

Fig. 2 shows the vibration modes of the bar for the following parameters: length = 691 mm, thickness = 3.04 mm, width = 15.9 mm, ρ = 2660 kg/m3 and E = 65.6 GPa. These amplitudes are normalized by their maximal values. We clearly see that the computed modes exactly match the experimental measurements obtained using a point-like source as well as a piezoelectric sensor glued on the bar. The only difference between the two source types appears in the amplitude of the considered mode. It is not visible on Fig. 2 because all the amplitudes are normalized to 1. The modes that are displayed on this figure are arbitrarily chosen according to a series of prime numbers less than 40. Mode 2 is not shown because it is below the frequency filter threshold of our measurement setup.

3 Influence of the physical contact

3.1 Deflection of a silicone material

The bar being in vibration, we now apply a local strength on it. The local contact with a viscoelastic material as the pulp of the human finger yields an attenuation of the vibration of the bar. In order to obtain reproducible measurements, the human finger pulp is replaced by a silicone material classically used for moulding and stable in time. Its Young modulus is 1.3 MPa, ten times larger than the Young modulus of biological tissues. The artificial finger has a cylindrical shape, it is illustrated on Fig. 1. The contact surface with the bar has a diameter of 10 mm, similar to a light contact of a human finger on a hard surface. The measurement of this diameter has been realized with a set of 10 students and researchers of the laboratory. The force applied by these persons for a so-called “light pressure” has been measured with a high-precision balance ; it varies from 30 g to 70g. Compared to an average contact surface of 78.5 mm^2, we finally obtain an average pressure between 5 and 8 mN/mm^2.

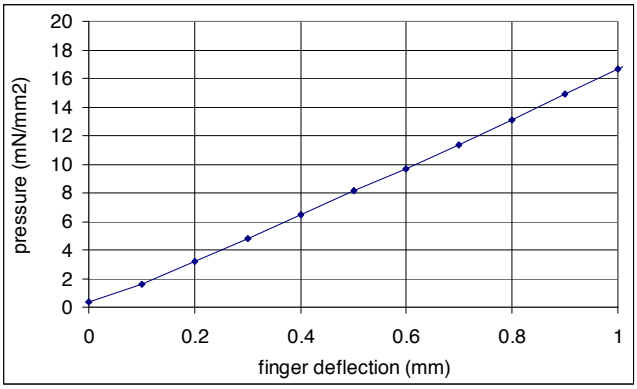

Figure 3: Pressure versus silicone finger deflection ; contact surface diameter: 10 mm.

Fig. 3 shows the variation of the pressure applied by the viscoelastic artificial finger with its deflection on the rigid surface. In order to obtain a pressure similar to the one corresponding to the so-called “light pressure” with the human finger, we choose a deflection of 0.5 mm measured from the contact position.

3.2 Deflection with the silicone finger

The artificial finger is now applied on different locations of the vibrating bar. The excitation is generated from the piezoelectric sensor. The laser vibrometer is located 1 mm from the left end of the bar ; this allows an efficient detection of all existing modes.

Fig. 4 represents the absorption of each mode (dashed and dotted lines) as a function of the position of the silicone finger along the bar. The vibration amplitudes are normalized by those measured without deflection nor contact of the finger. We see that the absorption changes in the opposite direction compared to the modes of the free bar (continuous lines). The absorption is maximum when the deflection is located at a maximum of the vibration of the bar, and minimum at a vibration node. For each mode, antinodes and nodes are located at different places on the bar, except on its middle (Fig. 1). In this particular case, two modes of orders separated by 2 correspond to either a node or an antinode. This figure also shows the reproducibility of the experiment, since two experiments realized at different times with different spatial steps (see dashed and dotted curves) yield well-correlated absorption curves.

From the results presented on Fig. 4, we can extract the absorption profiles for several positions of the artificial finger and for modes from 3 to 39 ; these absorption profiles are shown on Fig. 5. We observe that for a given position, the absorption differs from one mode to another one. This observation is reinforced by the auto-correlation of the modal absorption profiles of the artificial finger, shown on Fig. 6. Based on this experimental result, we can measure and keep in memory the modal absorption profiles for predefined positions ; it is then possible to know the position of any new finger contact by a very simple comparison. This allows to get a tactile behavior of the system. Of course, some difficulties remain due to the symmetrical geometry of the bar: two identical modal absorption profiles exist on both sides of the center of the bar.

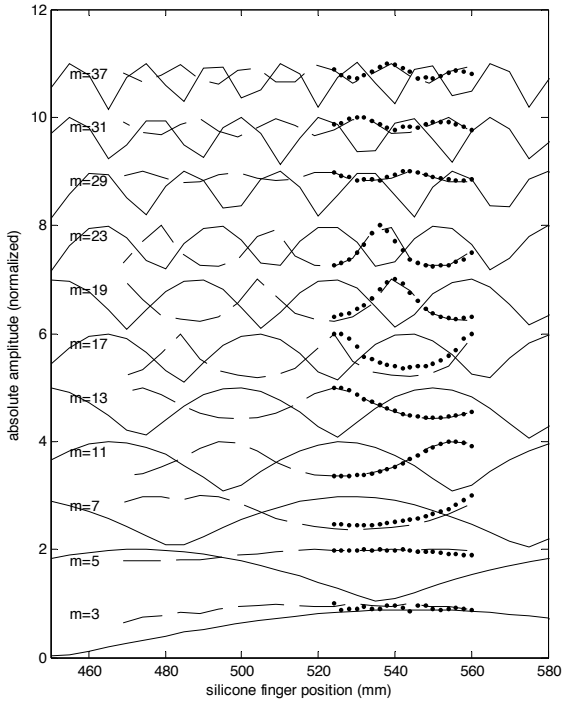

Figure 4: Attenuation patterns of arbitrary chosen modes versus position of the silicone finger (dotted and dashed lines) ; continuous lines represent theoretical free beam vibration absolute amplitudes.

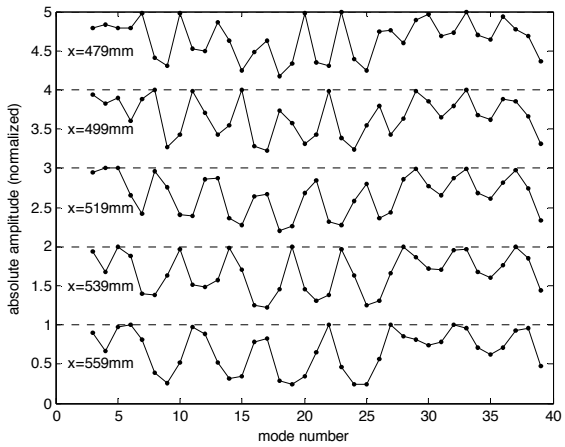

Figure 5: Attenuation pattern versus mode numbers for five positions of the silicone finger.

3.3 Deflection with a real finger

We now run the same experiment using a real human finger. The finger is either dry or wet by contact with a sponge before each deflection. Fig. 7 shows the maximal values of the cross-correlation between the modal absorption profiles obtained with the human finger and the ones obtained with the silicone finger. Although the contrast is a weaker than the one shown on Fig. 6, it remains usable and allows a correct determination of the position of the deflection with the real human finger, dry or wet. The maximal correlation are mostly larger than 90 %. This result may be surprising because the deflection strenght and the deformation of the finger pulp are experimental parameters that may change significantly in time and in contact position.

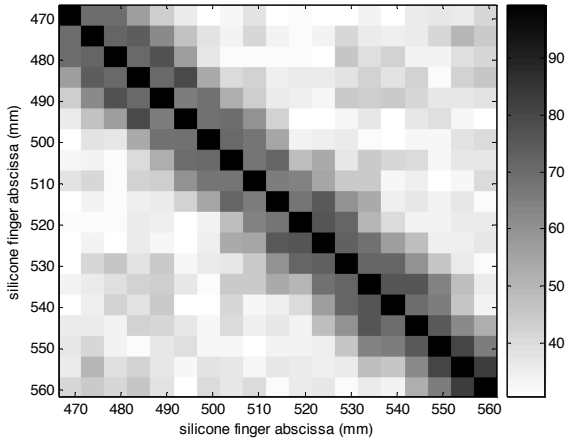

Fig. 6 Maximum auto-correlation values (%) of the modal absorption patterns of the silicone finger.

4 Conclusion

The system that has been developed is quite simple and allows, at least theoretically by extension of the principle, to use plates of any geometry as tactile objects, using only one emitter and one receiver, or even one single transducer that can work in the emitting and receiving modes. One significant advantage of this system is that the computation load is small in terms of the signal processing. The absorption profiles could even be quantified using two different levels, using a threshold of the normalized amplitude in an adequate manner. Then a binary comparator could be used to analyze fast any new absorption profile.

The problem of the symmetry of the plate can be solved, either using a geometry with no particular symmetry, or by introducing in the symmetric plate a small heterogeneity that would break the symmetry of the vibration modes, or by adding a static force measurement system at each corner of the plate in order to approximatively determine in which part of the plate the deflection has been applied.

(a)

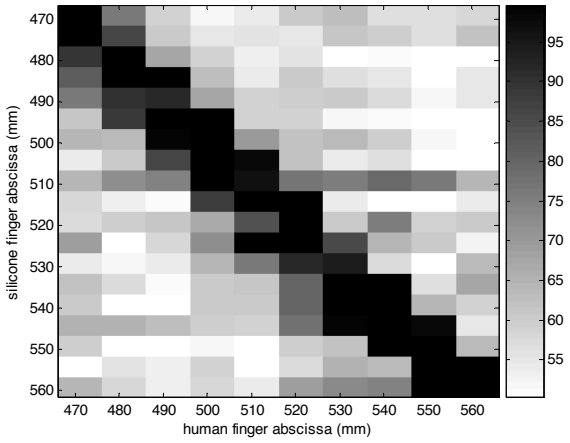

(b)

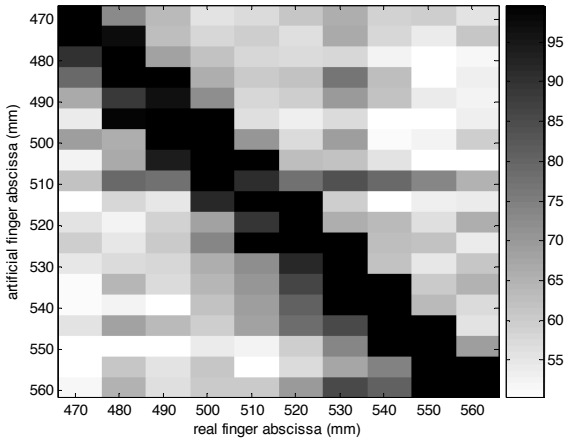

Fig. 7 Maximum correlation values (%) between modal absorption patterns of the silicone finger and the human finger. (a) and (b) corresponds respectively to dry and wet human finger contacts.

This work has started recently. In the next future, the absorption profiles with the silicone finger will be numerically modelled instead of being measured experimentally. Many numerical models have been published in the domain of damping of material structures by localized elastomer patches and can be of interest in the modelling of our problem. Moreover, similarly to Rayleigh or Love waves approaches of touch plate devices, the artificial finger should be optimized to have a behaviour as close as possible to the human finger. The results of these works will be published in the future.

References

[1] R. Johnson, U. S. Pat. 3,673,327 (1972)

[2] R. Adler and P. Desmares, An economical touch panel using SAW absorption, Ultrason. Symp. Proc., 289-292 (1985)

[3] J.P. Nikolovski and F. Devige, French Pat. FR0008372 (2000)

[4] R. K. Ing, N. Quieffin, S. Catheline and M. Fink, "In solid localization of finger impacts using acoustic time-reversal process", Applied Physics Letters vol. 87, 204104, pp. 1-3, 2005

[5] R. K. Ing, N. Quieffin, S. Catheline, M. Fink, "Tangible interactive interface using acoustic time reversal process", J. Acoust. Soc. Am. 117, 2560 (2005)

[6] F. Fahy, Sound and structural vibration: radiation, transmission and response, Academic Press, London, 1985